Benefits of using dense OBN for exploration: an example from Utsira using AI and machine learning

Sindre Jansen[1*], Adriana Citlali Ramirez[1], David Went[1] and Bezhad Alaei[2] demonstrate the benefits of using angle-rich, full-amizuth OBN data, and machine learning in the South Viking Graben.

Abstract

The first example of artificial intelligence (AI) geological interpretation on a large scale, densely sampled ocean bottom node (OBN) exploration dataset, Utsira OBN, is presented here. This entirely new suite of derivative seismic products provides enhanced exploration insights through AI, especially in areas where infrastructure led exploration (ILX) is drawing increased focus from the E&P industry. This work is complemented with a velocity model built with the latest processing technology: ultra-long offset and reflection FWI combined with tomography and anisotropy updates. The toolboxes, processing versus AI/ML, do not exclude or replace each other; a combined analysis can extract added value and reduce uncertainties. Such analysis is presented here.

Introduction

Derisking by amplitude versus offset (AVO) is common within the South Viking Graben. The Utsira OBN survey, located in this area, provides a wide-angle range allowing for accurate AVO. Its full-azimuth nature and ultra-high density provides high signal-to-noise ratio and rich frequency content, especially at the low end of the spectrum, which not only helps in the model building and imaging but in the stability of AVO.

The purpose of this paper is to demonstrate some of the benefits of angle-rich, full-azimuth OBN data. The analysis presented here focuses on Utsira OBN and uses:

1) The imaged cubes (full stack and angles stacks),
2) Well data within the area covered by the survey,
3) Machine learning (ML) and artificial intelligence (AI) well and seismic analysis, interpretation, and property prediction, and

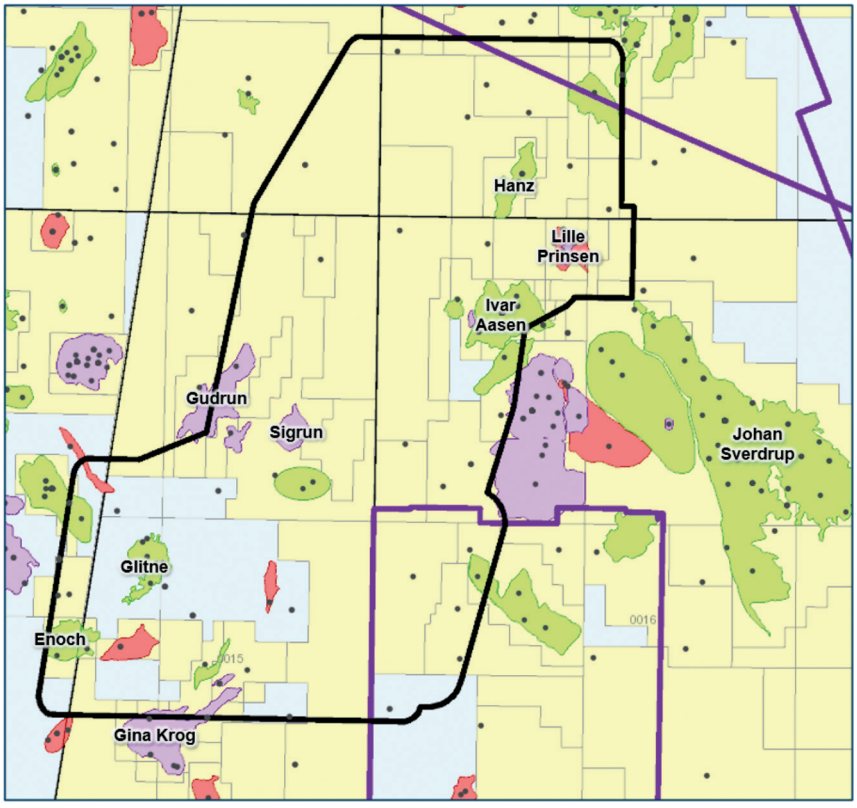

Figure 1 Outline of the Utsira OBN receiver carpet (black), active production licences (yellow), TGS data (purple) and fields and discoveries.

[1] TGS | [2] ESA
* Corresponding author, E-mail: sindre.jansen@tgs.com
DOI: 10.3997/1365-2397.fb2021074

Field	Reservoir challenge
Gina Krog – Mid Jurassic	Complex segmented reservoir with poor to moderate quality.
Gudrun – Mid to late Jurassic	Complex reservoir with moderate quality and key uncertainty relating to sand distribution and connectivity, especially within the Late Jurassic Draupne Fm.
Ivar Aasen – Late Triassic to Mid Jurassic	Segmented with moderate-to-good quality.
Enoch – Paleocene to Eocene	Varying reservoir quality.

Table 1 Producing fields, main reservoir interval and summary of reservoir challenges as listed on the NPD website.

4) A velocity model built using ultra-long offsets and reflection FWI.

The results of the AI/ML toolbox are shown to provide beneficial complementary views of the subsurface to those obtained by more standard methods (albeit modern) such as the velocity model built to image the data. The combination of toolboxes and analysis in this work aims at providing enhanced exploration insights, including observations that can help to derisk subsurface sedimentology and potential fluid content.

Utsira OBN and the survey area

During 2018 and 2019 AGS and TGS acquired the Utsira OBN survey in the South Viking Graben. The outline is in Figure 1 and represents the largest densely sampled OBN survey ever acquired for exploration purposes. The survey area covers more than 2000 km^2 across the Gudrun Terrace and parts of the Utsira High. It includes a variety of play models ranging in stratigraphy from Tertiary to Paleozoic basement.

The South Viking Graben is considered mature with four producing assets (Gudrun, Ivar Aasen, Gina Krog and Enoch) within the Utsira OBN survey area: Glitne, which has ceased production and is abandoned, and six discoveries likely to be put on production within the next 10 years. Exploration success within the survey area started in 1975 with the discovery of the Gudrun Field, which began production in 2014. Since 2000, the four producing assets combined with the shut-in Glitne Field have combined investments of approximately $11.6 billion (NPD 2021). The fields have produced more than 450 Mmbbl of oil equivalents. To maintain the economics of the projects and capitalize on the existing investments, the operators of these assets are expected to focus on enhancing production and exploring for nearby hydrocarbon accumulations with low-cost tie-back possibilities.

A good understanding of the reservoir is key for both enhanced production and successful exploration for hydrocarbon accumulations. Below, we list three contributing factors complicating the exploration and production activity within the Utsira OBN survey area. These challenges are interlinked and relate to:

Reservoir quality and connectivity: Gina Krog, Gudrun, Ivar Aasen, and Enoch all encounter uncertainties related to volume, reservoir quality, phase, and connectivity (see Table 1). Improved understanding of the reservoir can be achieved by using well information and integrating the observations with geophysical methods such as seismic interpretation, model building and inversion. To this we can add prediction based on ML and AI. Accuracy of the respective methods is directly linked to the quality of seismic data leading to the imaging challenge.

Seismic imaging: Conventional narrow azimuth streamer data is challenged by insufficient illumination of the subsurface targets contributing to residual free-surface and interbed multiples, dimming, pull-up/pull-down effects and migration artifacts – including accurate placement of intrusive sands also known as injectites or v-brights. The full-azimuth Utsira OBN survey is designed to minimize the subsurface imaging challenges observed within the area relating to shallow velocity contrasts in the quaternary channels, irregular high acoustic impedance injectites in the Tertiary, and complex fault patterns through all target levels.

Rock physics and AVO: AVO forms the basis for rock and fluid property prediction and is considered a key derisking tool in areas where target zones have measurable AVO effects like in the Utsira OBN area. AVO class IIp anomalies are commonly observed for HC-filled reservoirs, as predicted by forward models (Figure 2). As highlighted in the figure, angles in range 0 to 60 degrees are necessary to measure both the intercept and the elastic effect. Legacy vintage streamer data lacks zero angle measurements because the source is in front of the streamer and not above. In addition to this, limited streamer length and azimuth coverage restricts the far-angle measurements to a maximum ~45 degrees. OBN data offers a wider range of acquisition angles at full azimuth which allows for a more thorough evaluation of reservoir AVO effects including azimuthal anisotropy

In total, 70 vintage 3D seismic surveys intersect the Utsira OBN survey outline. Initially, exploration was done using 2D seismic data. In 1975, the first commercial 3D seismic survey was acquired in the North Sea (Davies et al., 2014). Later, 3D

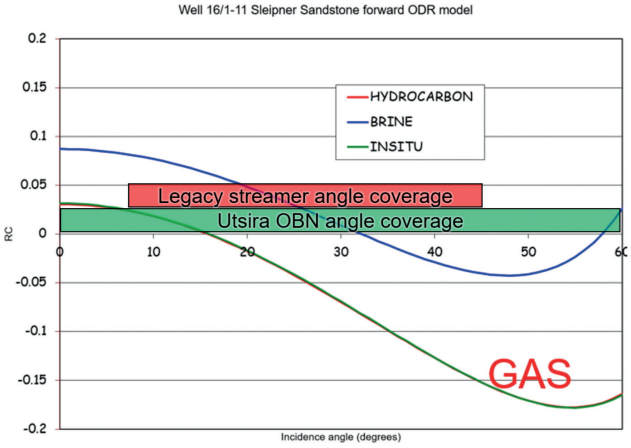

Figure 2 Forward model for gas vs brine-filled Sleipner Fm in well 16/1-11 (Ivar Aasen).

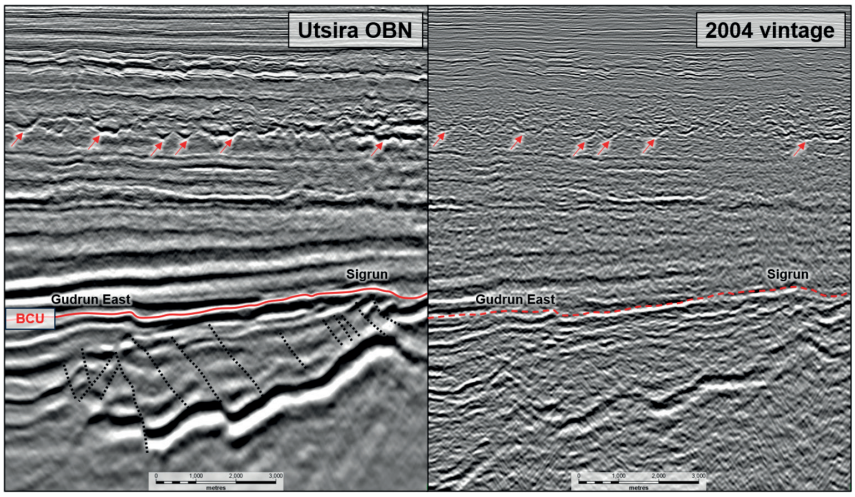

Figure 3 Example line through Gudrun East Field and Sigrun discovery comparing Utsira OBN (left) to a released 2004 3D streamer (right) and the respective imaging of injectites (red arrows) and complex faulting.

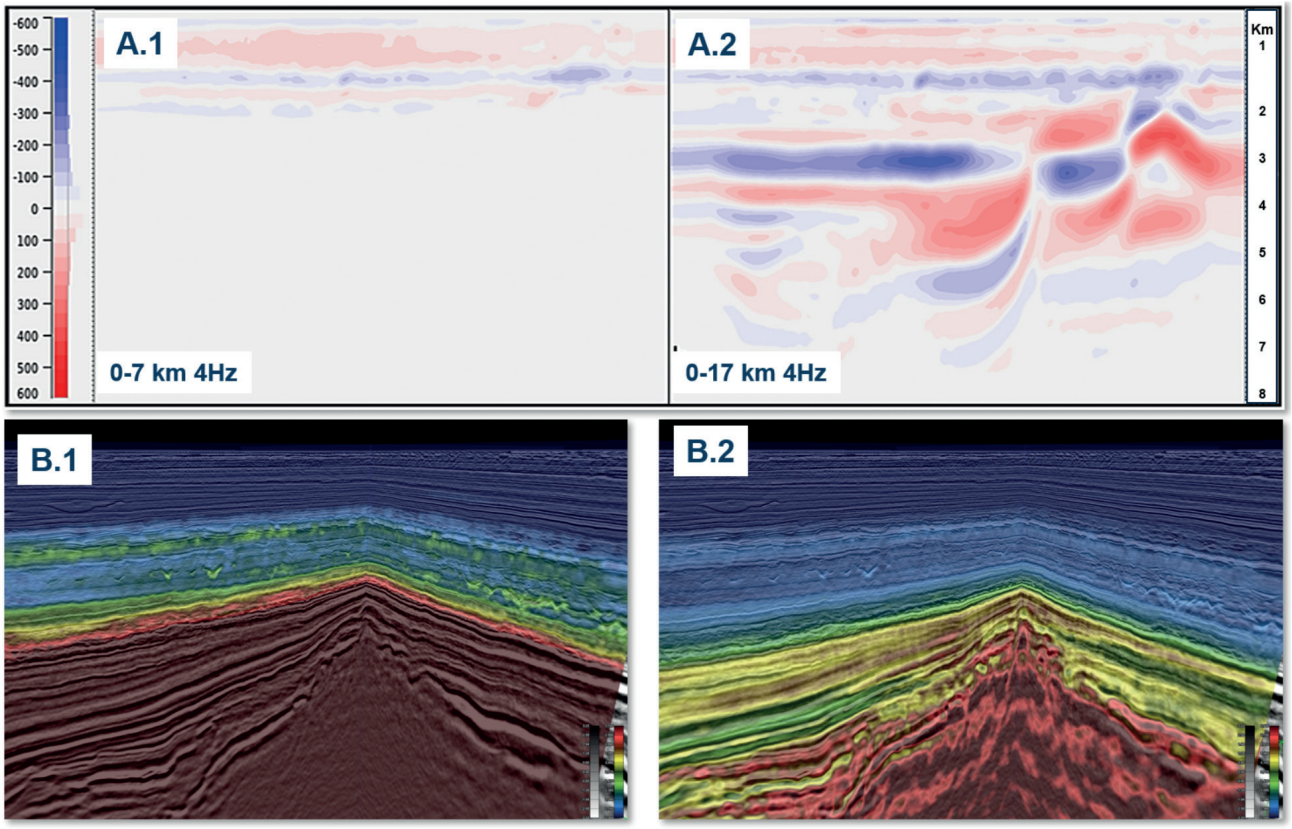

Figure 4 FWI-based velocity model using ultra-long offsets (17 km) and DM FWI. A.1 focusing on the colourbar range to emphasize the injectites, and A.2 focusing on the colourbar to illustrate the Mesozoic layering and faulting.

streamer seismic became standard, varying from narrow azimuth 3D surveys to more recently multi-azimuth streamer surveys. A split spread test (~200 km^2) was acquired in 2018. Conversely, full-azimuth OBN 3D seismic data in the area was limited to a 4D over the Ivar Aasen Field until the acquisition of the Utsira OBN. Figure 3 compares inlines from 2004 towed-streamer data and the Utsira OBN data. It highlights the significant improvements obtained through both acquisition and processing advances. The water depth is approximately 110 m and the seismic image shows the producing Gudrun Field and the Sigrun discovery at around 4 km depth.

The regional imaged cube was processed with modern technology, including FWI up to 5Hz, but with maximum offsets limited to 6.7 km. To extract further value from the Utsira OBN dataset, TGS has continued reprocessing using dynamic matching FWI (DM FWI). OBN surveys naturally measure ultra-long offsets that can be extracted from the data with deblending technology (offsets of up to 30 km were extracted after deblending). Utsira OBN was acquired in an area with a bathymetry averaging 110 m. A feasibility analysis and the FWI tests carried out by Ramírez et al. 2020, showed that the main diving wave contribution was contained within split-spread maximum offsets of 17 km. Thus, in the reprocessing, this offset range was used in a first pass of DM FWI that provided main updates to the velocity model down to ~5-6 km (depending on the geology, this velocity update can reach beyond 7 km). Figure 4A (top) is an example of the velocity

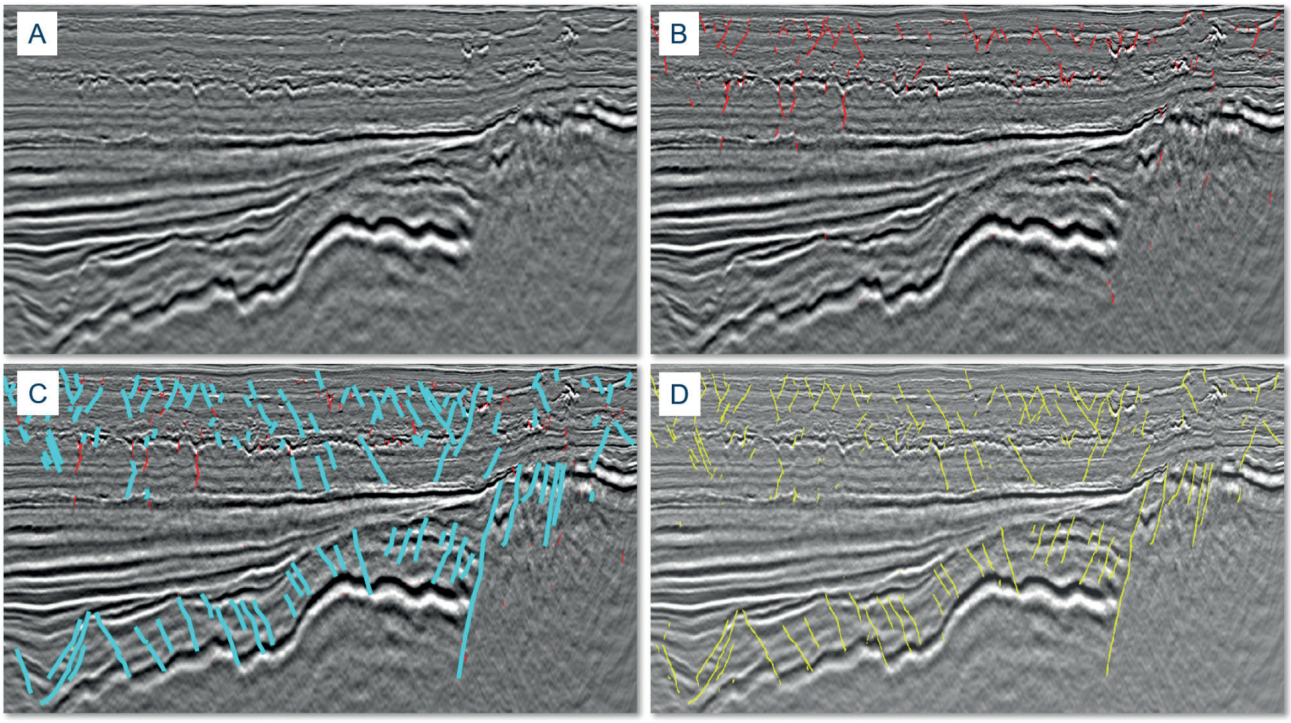

Figure 5 Utsira OBN inlines example (A), applying pre-trained fault model (B), additional interpretation/labelling (C), ML and output (D).

update (dV) after the first frequency band of FWI updates with diving waves, using offsets from 0 to 7 km (A.1) versus 0 to 17 km (A.2). Diving wave FWI was followed by tomography and anisotropy updates, and a reflection pass of DM-FWI. The goal of the model-building strategy was to extract a more accurate model than the regional one and to better characterize complex and high-contrast anomalies such as injectites. The latter DM FWI velocity model in Figure 4B (bottom) captures both velocity contrasts associated with the injectites (B.1) and the deeper Mesozoic layering and faults (B.2).

ML and AI for geobody and property prediction

Some 156 wells have been drilled within the Utsira OBN receiver area, and 106 of these are released. TGS and Earth Science Analytics (ESA) have initiated a ML/AI project on the Utsira OBN 3D survey. The project has three main objectives: fault and injectite modelling, missing well logs prediction, and 3D property prediction of Vp, Vs, density, and four lithology types. The outcome shows a good correlation when benchmarked against the Utsira OBN seismic interpretation, wells, and the DM FWI velocity model.

Methods

Fault and injectite modelling using ML

Structural seismic interpretation was performed on the Utsira OBN survey using ML methods within cloud-native EarthNET platform. The purpose was to output faults and injectite geobodies. The workflow followed a classical ML scheme, starting by applying a pre-trained fault and injectite model to the Utsira OBN data, followed by labelling (interpretation) and eventually training the models by ML to complete the exercise. Figure 5 shows an example from each fault modelling step leading to the final output model.

Missing well logs and 3D property prediction

Prediction of reservoir properties using seismic data can be carried out using ML (e.g. Sun et al., 2021; Wu et al., 2021). Figure 6 shows the workflow that we utilized to predict reservoir properties from OBN seismic data in this study.

We have then used 1D convolutional Neural Networks (CNN) to predict elastic and reservoir properties from OBN seismic data. The prediction accuracy depends on the quality of the labels, and seismic data as well as the network architecture. Deep learning algorithms require enough data (in this case number of wells used in training) to build successful models to predict target properties. In order to provide good quality labels for training with high coverage, we have performed ML on well data to predict both elastic and reservoir properties (first part of the workflow, Figure 6), to fill in gaps, and increase the depth coverage of logs that are used as labels or targets in seismic-scale property prediction.

Upscaling logs from well scale to seismic scale has been tested using different approaches. For elastic logs, lowpass

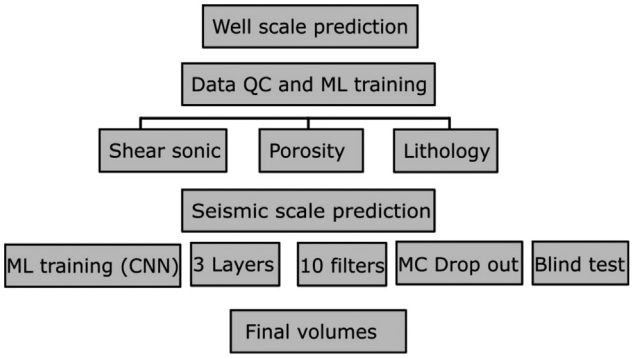

Figure 6 Workflow used to predict reservoir properties from wells and the Utsira OBN data. Monte Carlo (MC) drop out applied in the model training.

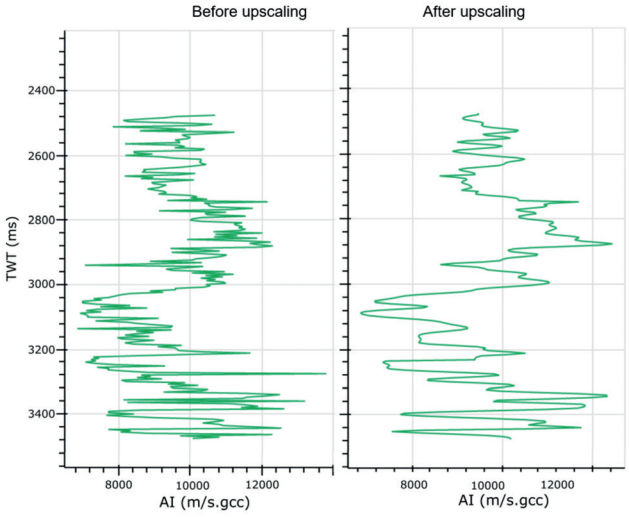

Figure 7 Acoustic Impedance log in a well before (left) and after (right) a low pass 40Hz filter.

filters as well as Backus averaging were tested. The dominant frequency of the OBN seismic data at target intervals was used as an indication to set the upscaling parameters. Figure 7 shows an example of an acoustic impedance log in one of the wells before and after a low pass 40Hz filter. We sliced the seismic data around wellbores to generate training sets from seismic volumes. Immediate neighbouring trace or traces around the wellbore were selected at each depth/time. The radius or number of traces around the wellbore was used as a parameter to build the seismic training data for each well. An important point to consider when adding more traces around the wells was structural complexity at wellbore location.

From the regional Utsira OBN deliverables (2020), seven features were used for training in this study including one interval velocity volume, full-stack and five angle stacks.

The deep neural network architecture used in the training process is 1D CNN and it has 3 layers (Figure 6) and 8 to 12 filters. The hyperparameters used for most of the training examples are a batch size of 64 and 32 samples, 256 and lower samples for each sequence, 0.1- 0.2 noise. A range of 200 to 500 epochs was used in the training. For model hyperparameters tuning, three options were available including random search, hyperband, and Bayesian optimization. The main loss-function used in the training was mean square error. However, several other loss-functions such as log cosh function, Huber loss, mean absolute error were available. RMSprop, ADAM, and NADAM optimizers were tested and used for different training sets. The option to give higher weight to model optimization in target formations was also used. Finally, we built blind models using one well held out to verify the performance of each model.

Figure 8 shows an example of acoustic impedance training and the predicted results along an inline crossing the well.

Results

Fault and injectite modelling

The legacy EarthNET fault and injectites models were trained using released 3D streamer seismic data from Diskos, with no previous experience on full-azimuth OBN data. Despite this fact, Figure 5B shows that the pre-trained model initially picked a high concentration of the Eocene and Tertiary polygonal faulting highlighted with red fault sticks. An interpretation of these faults, also highlighted in Figure 9.A, is important because they may provide migration pathways for hydrocarbons (Lonergan et al. 1999). Studies also suggest their absence in certain areas may indicate underlying sands**.**

Due to the nature of the OBN data compared to the streamer data, additional labelling and ML was required for the deeper Mesozoic faults. Labelling of five inlines and crosslines before ML provided a fault model for the deeper Mesozoic. The labelling process is shown with blue fault sticks in Figure 5C and the final after ML is shown with yellow fault sticks in Figure 5D. The Mesozoic faults are important to understand for compartmentalization, migration pathways, structural regimes and their implications on sediment transport.

We have identified two main intervals of Tertiary intrusive injectites based on cross-cutting relationships and stratigraphic thicknesses within the South Viking Graben. The first event of injectites likely occurred in the Late Eocene period and intruded Mid-Eocene strata, and the second event occurred around late

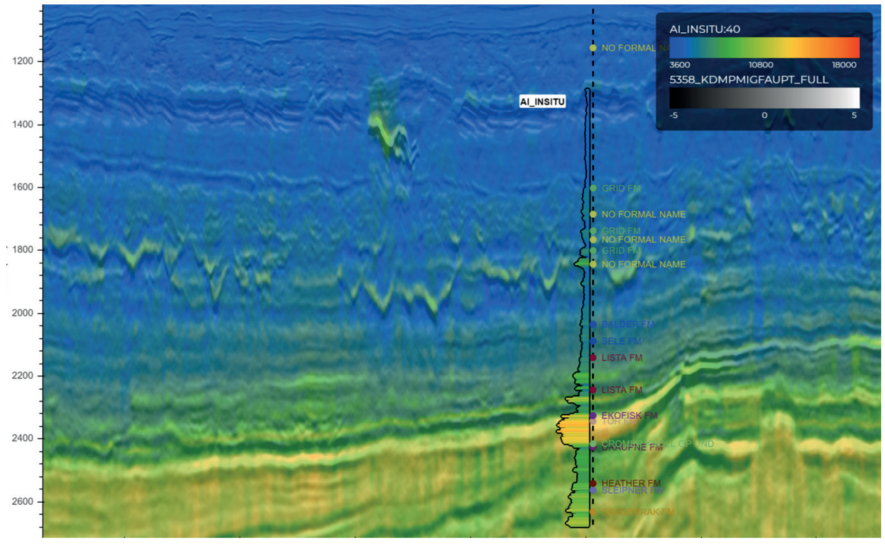

Figure 8 Example from acoustic impedance training and predicted results along a well.

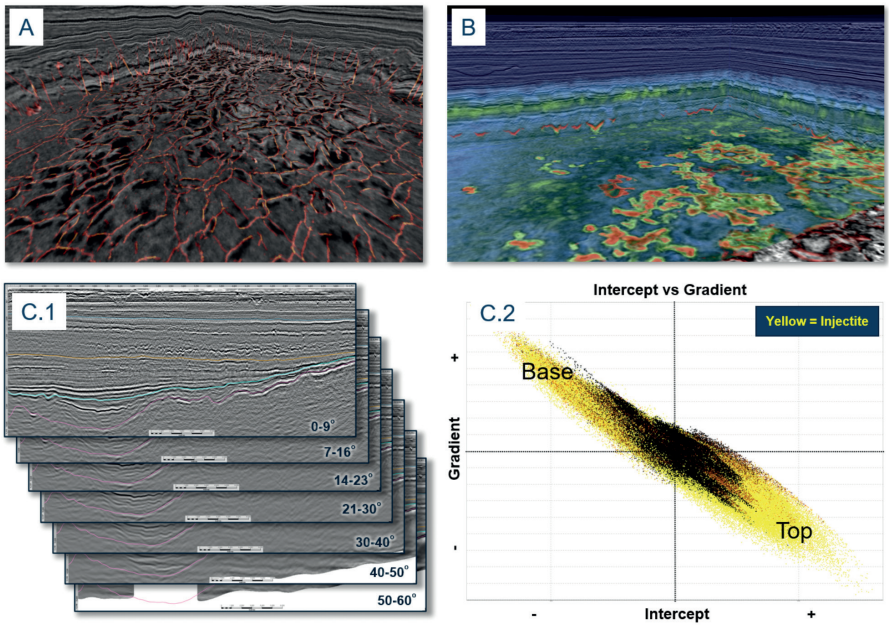

Figure 9 Modelled faults (A), injectites (B, red) overlain DM FWI velocity model, Utsira OBN angle stacks (C.1) and intercept versus gradient plot of modelled injectites (C.2).

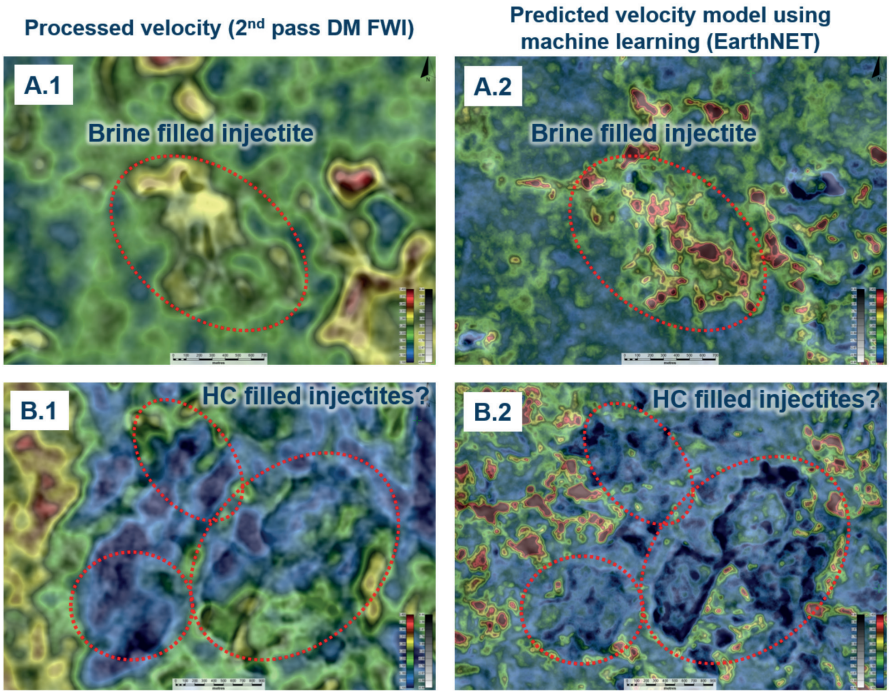

Figure 10 Depth slices(~1600 m) comparing brine-filled injectites (A) and possible HC-filled injectites (B) using DM-FWI velocity model (1) and ML-predicted velocity model (2).

Oligocene period and intruded Mid-Eocene strata. Generally, brine-filled injectites show high acoustic impedance contrasts relative to the surrounding host rock, leading to a hard-to-soft seismic response at top-to-base, respectively. Changing the fluid content from brine to hydrocarbons lowers the velocity and density, affecting the resulting seismic response. Figure 9.B shows that the processed DM FWI velocity model captures velocity anomalies associated with the injectites, and the ML-modelled injectites highlighted in red support their presence. Manual interpretation of the injectites would be extremely time consuming due to their high concentration, while modelling using ML proves to be efficient and effective.

Figure 9C.1 shows the Utsira OBN angle stacks from 0 to 60 degrees. Angle stacks have been used to calculate the intercept versus gradient plot in Figure 9C.2. It illustrates the strong acoustic impedance contrast associated with the top of the injectites by a positive-intercept-negative-gradient response. The base of the injectites have been modelled shown with a negative-intercept-positive-gradient response.

Several wells have encountered brine-filled injectites. Prospective injectites remain under-explored with only one discovery in the Utsira OBN area. Figure 10 compares the DM FWI velocity model to the velocity model predicted using ML and AI. The depth slices intersect a drilled brine-filled injectite (A.1 and A.2) and lower velocity injectites (B.1 and B.2) in an area of possible HC-filled injectites. Both the DM FWI (left) and AI-predicted velocity model (right) support observations indicating higher velocity associated with unprospective injectites.

Predicting Eocene channel sands

The Grid Formation within the Hordaland Group was deposited during Mid to Late Eocene, and partly consists of amalgamated sand bodies likely to be derived from the East Shetland Platform (NPD, 2021). It is shown in Figure 11A.1 as a package with generally poor continuity on full-stack data. Several wells have penetrated the Grid Formation channel sands. The well used in Figure 11 and Figure 12 measures an average sand porosity of 35% and represents a blind test in the AI property prediction.

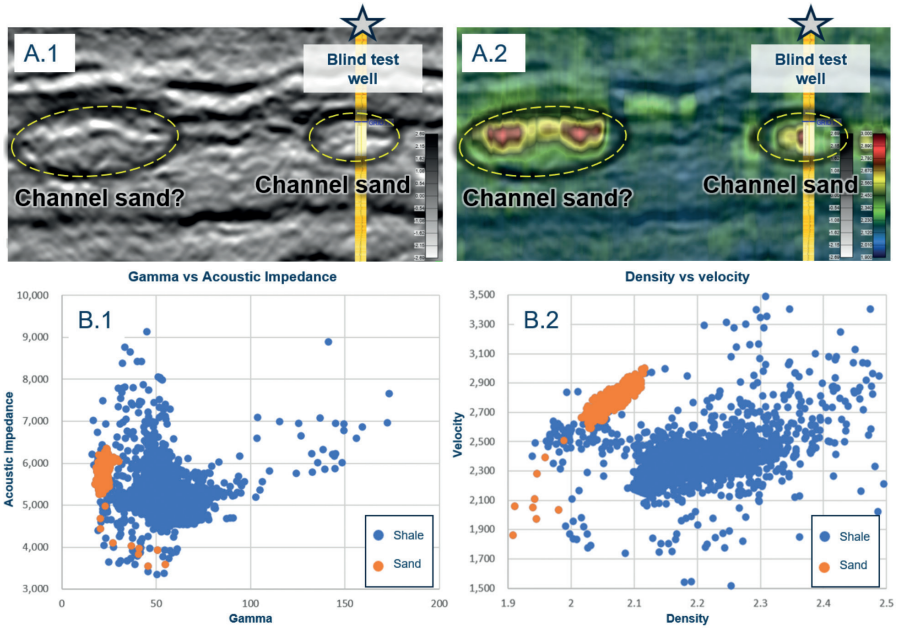

Figure 11 Utsira OBN full-stack line example (A.1) intersecting the blind test well penetrating Grid Fm channel sand. Crossplots show the logged Grid Fm sand velocity vs density (B.2), and the logged gamma vs calculated acoustic impedance (B.2).

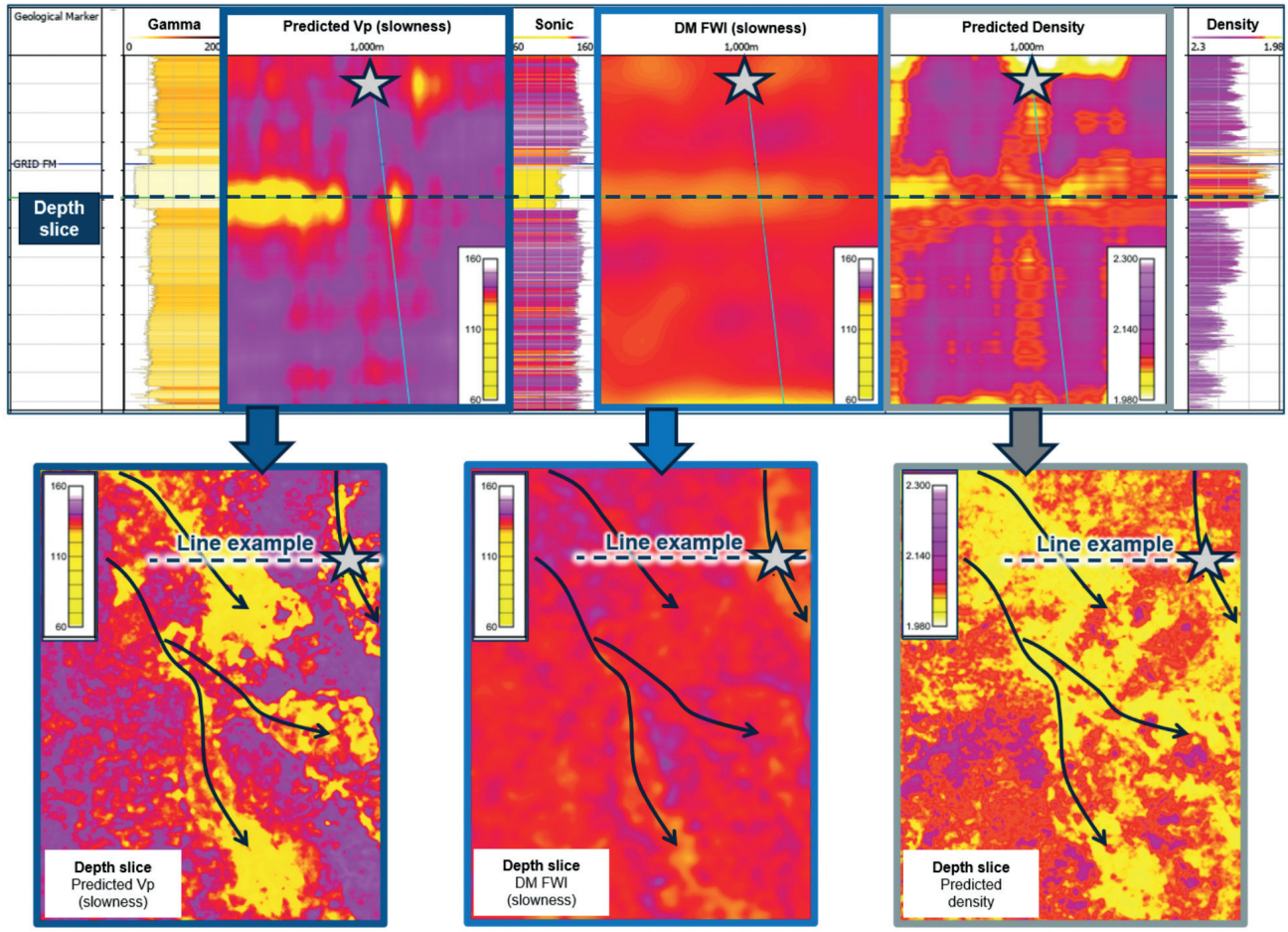

Figure 12 Top figure shows the blind test well in Figure 11 with measured gamma, sonic and density. The respective AI-predicted properties are highlighted along the well bore (top) and depth slice through the penetrated channel (bottom) using the same colourbar.

A crossplot of the Grid Formation velocity versus density from the blind test well logs (see Figure 11B.2) shows good discrimination between sand and shale. The sand generally has higher velocity (2650m/s to 2950m/s) and lower density (2g/cm3 to 2.1g/cm3) than the silt and shale. However, a crossplot of the calculated acoustic impedance versus gamma in Figure 11B.1 shows a poor discrimination between the sand and shale, partly explaining the poor continuity of reflectors when using full-stack data. It also emphasizes a need for using AVO, velocity and density volumes when interpreting these sands. Figure 11A.2 shows an AI-predicted Vp anomaly over the penetrated channel with similar velocity (2650m/s to 2950m/s) as shown in the blind test well. Another anomaly showing similar velocity is located west of the well location in Figure 11A.2, indicating presence of a larger undrilled channel. In the next paragraph, we investigate this further.

In Figure 12 (top), we show the blind test well described below with gamma, sonic and density logs around the Grid Formation channel. The AI predicted properties and the DM FWI is shown in parallel panels to the measured logs with the same colourbar. There is a strong correlation between the AI-predicted Vp and the sonic log. By comparing the DM FWI to the sonic and predicted Vp, we see a velocity anomaly associated with the penetrated channel in the DM FWI. However, as expected the DM FWI velocity resolution is less sharp. In map view shown in Figure 12 (bottom), we see the AI-predicted Vp and density outline the penetrated channel. The DM FWI depth slice supports this observation, though not in the same detail as highlighted by the predicted Vp and density. Further to this, we can see several other anomalies west and south of the well location, indicating the presence of more channels.

A strong correlation between what is measured in the blind test well, DM FWI velocity volume and the AI predicted Vp and density highlights the ability of the Utsira OBN to accurately map the Grid Formation sandstones.

Conclusion

Within this study an integrated approach to derisking sand presence and also fluid type is presented. The study area lies within the mature South Viking Graben, Norwegian North Sea, dominated by infrastructure-led exploration (ILX). The study incorporates use of dense OBN data in an area dominated by numerous streamer vintages, combined with artificial intelligence and machine learning-driven interpretation and property predictions.

The conclusion can be summarized in three main points:

1) The dense OBN survey provides azimuths, angles and offsets which have previously not been measured in the area. It has been shown that the OBN acquisition solution allows for improved imaging of subsurface exploration targets, such as Tertiary injectites and Jurassic fault blocks. It is well known that all angle ranges are important for AVO, but more so are zero offsets for intercept and acoustic impedance measurement, and far angles for the elastic effects. The work presented here is an example of how relevant the angle coverage is for derisking HC-filled Jurassic reservoirs with an AVO Class IIp response, and also low acoustic impedance Eocene sands. Reprocessing dense OBN data using 17 km offsets and dynamic matching full waveform inversion (DM FWI) provide a detailed velocity model down to 6 km, enabling derisking Tertiary injectite fluid content and Eocene reservoir sand presence – both of which have been limiting risk factors when exploring using conventional streamer data.
2) Injectite and fault modelling using the cloud-native EarthNET platform has proven robust and efficient, yielding accurate models for improved understanding of migration pathways, compartmentalization, and reservoir presence.
3) AI and ML property predictions of Vp and density using wells and the OBN dataset show high accuracy when compared against wells and the DM FWI velocity model. Strong capabilities of derisking Eocene channel sands have been demonstrated by benchmarking the results against a blind test well and the DM FWI velocity model.

Future work will include finalizing AI and ML property predictions of shear wave (Vs) for fluid detection, and also facies to further derisk the reservoir presence. Reprocessing the OBN data using recorded shear wave will aim to provide a complementary dataset to the property predictions and further derisking of the subsurface in the study area.

References

Davies, J., Stewart, A., Cartwright, A., Lappin, M., Johnston, R., Fraser, I. and Brown, R. [2004]. "3D Seismic Technology: Are We Realizing Its Full Potential", Geological Society, London, Memoirs, 1-10.

Lonergan, L. and Cartwright, L. [1999]. Polygonal Faults and Their Influence on Deep-Water Sandstone Reservoir Geometries, Alba Field, United Kingdom Central North Sea, *AAPG Bulletin*, **83**(3), 410-432.

Ramirez, A., Baldock, S., Mondal, D., Gromotka, J. and Hart, M. [2020]. Long offset ocean bottom node full-waveform inversion and multi-azimuth tomography for high-resolution velocity model building: North Sea, Utsira High, SEG Technical Program Expanded Abstracts 2020. https://library.seg.org/doi/10.1190/segam2020-3428806.1.

Sun, J., Innanen, A.K. and Huang, C. [2021]. Physics-guided deep learning for seismic inversion with hybrid training and uncertainty analysis, *Geophysics,* **86**, R303-R317. https://doi.org/10.1190/geo2020-0312.1.

The Norwegian Petroleum Directorate (NPD) 8. Aug 2021, https://factpages.npd.no/nb-no/field/PageView/All.

The Norwegian Petroleum Directorate (NPD) 8. Aug 2021, https://www.npd.no/contentassets/f0bf7cf3f3ee4700b9a361e2e9351369/chapter-4.pdf.

Wu, X., Yan, S., Bi, Z., Zhang, S. and Si, H. [2021]. "Deep learning for multi-dimensional seismic impedance inversion," *Geophysics,* **0**, 1-44. https://doi.org/10.1190/geo2020-0564.1.

Zoeppritz, Karl [1919]. "VIIb. Über Reflexion und Durchgang seismischer Wellen durch Unstetigkeitsflächen." [VIIb. On reflection and transmission of seismic waves by surfaces of discontinuity], Nachrichten von der Königlichen Gesellschaft der Wissenschaften zu Göttingen, Mathematisch-physikalische Klasse, 66-84.

Kohonen, T. [2001]. Self Organizing Maps. Third extended addition, Springer Series in Information Services, Vol. 30.

Leal, J., Jeronimo, R., Rada, F., Viloria, R. and Roden, R. [2019]. Net reservoir discrimination through multi-attribute analysis at single sample scale, *First Break*, **37**, 77-86.

Qi, J., Lyu, B., Alali, A,. Machado, G., Hu, Y. and Marfurt, K.J. [2019]. Image processing of seismic attributes for automatic fault extraction: *Geophysics*, **84**(1), O25-O37.

Qi, J., Machado, G. and Marfurt, K.J. [2017]. A workflow to skeletonize faults and stratigraphic features: *Geophysics*, **82**, O57-O70.

Qi, J., Zhang, B., Zhou, H. and Marfurt, K.J.[2014]. Attribute expression of fault-controlled karst–Fort Worth Basin, TX: Interpretation, **2**(3), SF91–SF110.

Qi, J., Lyu, B., Wu, X. and Marfurt, K.J. [2020]. Comparing convolutional neural networking and image processing seismic fault detection methods:90th Annual International Meeting, SEG, Expanded Abstracts, 1111-1115.

Radoil (Reel Power International Subsidiary) & Harris Pye Engineering, [2015]. Cheleken Contract Area Development, Caspian Sea, https://www.offshore-technology.com/projects/cheleken-contract-area-development-caspian-sea/.

Roden, R., Smith, T. and Sacrey, D. [2015]. Geologic pattern recognition from seismic attributes: Principal component analysis and self-organizing maps. *Interpretation*, B., SAE59-SAE83.

Ronneberger, O., Fischer, P.and Brox, T. [2015]. U-Net: Convolutional networks for biomedical image segmentation: International Conference on Medical Image Computing and Computer-Assisted Intervention, 234-241.

Van Dijk, J., Temitope Ajayi, A., Eid, T., Eldali, M., Ellen, H., Guney, H., Hashem, M., Knispel, R., Rouis, L. and Santoni, S. [2018]. An Integrated Geological Model for the Greater Cheleken Area Central Caspian Basin, Turkmenistan; Complex Synsedimentary Transcurrent Faulting and Compartmentalization in Plio-Pleistocene Clastic Reservoirs: presented at the Abu Dhabi International Petroleum Exhibition & Conference, https://doi.org/10.2118/192978-MS.

Wu, X., Liang, L., Shi, Y. and Fomel, S. [2019]. FaultSeg3D: Using synthetic data sets to train an end-to-end convolutional neural network for 3D seismic fault segmentation: *Geophysics*, **84**, IM35-IM45.

Zhao, T. and P. Mukhopadhyay, [2018]. A fault-detection workflow using deep learning and image processing: 88th Annual International Meeting, SEG, Expanded Abstracts, 1966-1970.